Preprints of the 19th World Congress
The International Federation of Automatic Control
Cape Town, South Africa. August 24-29, 2014

Topology Optimization of Porous Lattice Structures for Orthopaedic Implants

Geoffrey W. Rodgers*, Elijah E.W. Van Houten, Rohan Jean Bianco***, Romain Besset**** and Timothy B.F. Woodfield*****

**Dept. of Mechanical Engineering, University of Canterbury, Christchurch, New Zealand*
(e-mail: geoff.rodgers@canterbury.ac.nz).
***Professeur Agrégé, Université de Sherbrooke, Quebec, Canada*
(e-mail: eew.vanhouten@usherbrooke.ca)
**** Dpart. de Gnie Mcanique, Lcole Polytechnique de Montral, Montal, Canada,*
***** Supméca, Paris, France,*
****** Dept. of Orthopaedic Surgery & MSM, University of Otago, Christchurch, New Zealand*

Abstract: Porous lattice structures are finding increasing applications across a variety of scenarios, including industrial and medical uses which require precise structural characteristics such as stiffness, porosity, volume fraction and surface area. In many cases, a non-uniform distribution of these properties may be required to suit design requirements or to match *in-vivo* conditions in biomedical applications. In these situations, the design of the porous lattice can be quite complex due to competing objectives from the various distributed structural characteristics. Here we present an optimized structural design methodology that relies on global objective functions for effective stiffness, porosity, volume fraction and surface area.

1. INTRODUCTION

Low density porous structures can be found widely in nature, such as the trabecular bone, the structure of wood and many other growing organisms (Butterfield 1980; Steele 1988; Vincent 1990; Gibson 1997; Prendergast 2001; Li 2011). With the development of technology and science, man-made porous materials have been manufactured in large scale and attracted significant interest. Numerous processing routes have been developed to manufacture porous structures from materials, such as Al, Ti, Mg, ceramics and polymers (Ashby 2000; Montanini 2005; Ashby 2006). As a new class of materials, porous structures offer properties that no other monolithic materials can. They can be low density while having properties such as high mechanical strength, stiffness and damping capacity. For certain applications where a high surface area to volume ratio is important, only porous structures can satisfy the requirements. More importantly, they can be tailored to meet design or application requirements via changing structural variables (Ashby 2000; Lefebvre 2008). Applications of porous foams are across a wide range of industries, including electrical, aeronautical, automotive, building construction, military and medical fields (Asholt 1999; Ashby 2000; Banhart 2000).

While many of these porous structures (or foams) are commercially available, it is their application in orthopaedic devices and tissue engineering fields that has attracted more recent attention (Alvarez 2009; Hollister 2009). The porous architecture is known to facilitate tissue growth and implant fixation, as well as support flow of tissue fluid carrying nutrients (Woesz 1008; Hollister 2005; Armillotta 2008). Furthermore, porous structures have advantages of being sufficiently strong to provide suitable mechanical properties for the implanted site, while remaining lightweight.

For scaffolds to be used in load bearing applications, the structure needs to possess suitable mechanical properties to support the affected area, promote tissue growth, and allow integration and remodelling with host tissue to be established. The desirable mechanical properties should match those of the implanted region in terms of stiffness and strength to prevent stress-shielding problems. Stress shielding is one of the biggest concerns for load-bearing biomaterials, which occurs when the stiffness of the orthopaedic device is different from that of the surrounding or integrating bone, and leads to an uneven stress distribution between the bone and the implant. If the stiffness of the implant is higher than that of bone, the stress in the surrounding bone will be lower than usual and can cause bone resorption and loosening of the implant. In the opposite case, if the implant is not sufficiently stiff, micro-motion can cause fibrous encapsulation and loosening at the implant-bone interface, or potential implant failure due to higher stress concentrations (Pietrzak 1996; Wintermantel 1996). Stress shielding can affect bone remodelling and normal healing processes since under-loaded bone will adapt to the low stress environment and become more porous and weak (Rashmir-Raven 1995). For these reasons, porous structures, with controllable mechanical properties close to that of native bone, have the potential to minimise the risk of stress shielding (Staiger 2006; Witte 2007).

With ordered porous scaffolds, the pore architecture can be accurately designed and reliably controlled to be completely interconnecting throughout. This helps promote nutrient diffusion as well as cell and vascular infiltration, resulting in an improved bone formation over a broad range of pore sizes (Hollister 2005; Hollister 2005). This further confirms the advantages for developing optimisation porous lattice structures (OPLS).

This manuscript presents the development of an optimisation routine that minimises a weighted objective function that takes into account residual terms that represent deviations from target values for the stress profile, material volume fraction, and porosity. Different weighting factors are utilised to place varying importance on the different error terms and control the profile of the final solved geometry. A parametric study is presented to demonstrate the different geometry that is produced by the different weighting factors. Results are presented to show the output stress profile and representative indicators of material volume and porosity. Synthetic stress profiles are generated to test the robustness of the optimisation algorithm.

One specific application of optimised structures is the development of implants for replacement human inter-vertebral discs (IVD). For many patients that have suffered back injury or degeneration of the IVD, a bio-compatible implant is an important treatment technique. The optimisation routine is applied to measured values determined from experimental measurements on cadaveric human IVDs.

2. METHODS

2.1 Finite Element Model

The non-linear shape optimisation algorithm is formulated around a 3D finite element beam model to calculate the structural properties of the porous lattice. For the geometry determined by the optimisation routine, a finite element calculation is used to determine the resulting stress profile, while porosity and material volume calculations provide additional feedback to the optimisation routine.

The initial geometry is assumed to be a cubic grid of elements with constant element length. The regular grid is then mapped with orthogonal 3D beam elements whose cross-sectional area can be modified to alter the stiffness of the scaffold. A Timoshenko beam element formulation is used to account for shear deflections, due to the relatively squat aspect ratio of the individual beam elements.

2.2 Input and output parameters

A 3D lattice of beam elements defines the finite element model. The input into the model is a fixed strain profile at specified surface locations and the output is the resulting stress distribution at those same locations. The input strain values can be either synthetically generated or obtained from measurements of a physical system. The output stress profile from the finite element code can then be compared to the target stress profile to provide an indication of the suitability of the current geometry. The porosity and material volume are also calculated to guide to search algorithm.

2.3 Geometry manipulation

A 3D porous scaffold can have a very large number of individual elements. For example, a 3x3x3 scaffold, consisting of a matrix with three beam elements in each direction, will have a total of 144 beam elements. Similarly, a 5x5x5 matrix will contain 540 beam elements, while a 7x7x7 will contain 1344 beam elements. Therefore, it is necessary to reduce the number of independent variables to restrict the domain of the optimisation routine.

To achieve this objective, all beam elements are assumed to have a square cross-section, giving each element a single width parameter to be modified by the optimisation routine. The material elastic modulus and Poisson's ratio are assumed to be constant and known, as the entire scaffold is to be constructed from a single material. The overall number of parameters to be treated by the optimisation routine is thus equal to the total number of elements within the scaffold. By modifying the width of the cross-sectional area, both the axial and flexural stiffness of an element can be modified and the mechanical behaviour of the lattice is determined. The optimisation routine is used to derive an updated geometry for further analysis.

2.4 Optimisation objective function

The objective function is a weighted sum of terms representing porosity, material volume and surface stress values. The porosity term is included as this represents the ability of the scaffold to permit blood-flow, allowing for nutrient supply to the tissue to allow bone growth and osteo-integration of the implant. The porosity term is non-linear with pore size as it is related to capillary action of the biological fluid within individual ducts created by the porous scaffold. The material volume is included as an overall indicator of scaffold density, independent of fluid dynamics or capillary action. Finally, the stress error is used as it represents the ability of the scaffold to simulate the natural stress profile imparted into bone in the region of an artificial implant, promoting healthy bone density and avoiding stress shielding.

The overall objective function is defined as:

$$\Phi = \alpha(stress\_error) + \beta\left(\frac{|Porosity_{opt} - Porosity|}{Porosity_{opt}}\right) + \gamma\left(\frac{|Volume_{opt} - Volume|}{Volume_{opt}}\right) \quad (1)$$

where α, β and γ are the weighting factors that represent the relative importance of the stress error, porosity error and volume error respectively. By altering the relative magnitude of these terms, the resulting geometry can be modified to more closely match the target on any of these input variables.

The stress error is the sum of the stress errors for each element situated on the surface specified for stress optimization. The total stress error is the sum of the individual stress error for all surface elements and is defined:

$$stress\ error = \sum_{elm=1}^{N} \frac{\left| stress_{opt} - \left| \frac{reaction_{elm}}{A_{elm}} \right| \right|}{stress_{opt}} \quad (2)$$

where $stress_{opt}$ is the target stress value for that element, $reaction_{elm}$ is the calculated reaction load for that element and A_{elm} is the cross-sectional area of that element.

The stress error is represented within the optimisation routine as a single variable. However, the final resulting stress profile can be better represented by providing a colour grid plot of the target and actual stress profiles, showing the entire stress profile across the specified surfaces of the lattice, rather than simply a single number representing an aggregate stress match for the scaffold.

The optimisation routine utilises a conjugate gradient method for guiding the geometry modification to minimise the objective function. Specific details of the optimisation routine are not provided here due to space limitations (Shewchuk, 1994).

3. RESULTS

3.1 Input Parameters

Initial application of the topology optimisation method to porous biomaterials was done through the formation of cubic lattice structures with the same number of elements in all three dimensions. Each element or 'strut' of the lattice is a constant length and the cross-section is square. The edge length of the cross-section is modified individually by the optimisation routine to define to best topology to meet the design goals of the objective function. The length of each element within the cubic lattice structure is 2mm and the edge length of the cross-section is bounded to be a minimum of 0.6mm and a maximum of 1.6mm. The material used for the simulations is defined to be Titanium, due to the biological nature of the application, with Young's Modulus of 110GPa and a Poisson's ratio of 0.34. Initially, simulations are performed for cubic lattice structures with 3x3x3, 5x5x5 and 7x7x7 elements, giving a total number of elements of 144, 540 and 1344 respectively.

Initially, to utilise the optimisation routine and verify the output, synthetic target stress and strain profiles are used. Strain profiles are input as downward displacement boundary conditions on the top face of the implant, whereas stress profiles are pre-defined and incorporated into the optimisation routine. The boundary conditions of the lower face of the implant are fully fixed. While this investigation focuses solely on fixed boundary conditions on the bottom face and a target stress profile on the top face of the implant, there is nothing specific within the optimisation code to prevent alternate boundary conditions. Is it just as viable to apply loading on a side face of the implant or to apply a shear loading to the top.

At each iteration of the simulation, the current stress profile on the top face of the implant is calculated and the stress error between the current and target stress profile is calculated according to Eq. 2. The overall porosity and material volume fraction are also calculated and included into the objective function by their respective weighting factors. The topology is then iteratively modified to minimise the objective function.

A variety of optimisation simulations was undertaken for different stress profiles. Uniform strain profiles are input as boundary conditions and the topology was optimised with the goal of matching a target stress profile: uniform; linearly varying; and parabolic. This collection of stress and strain profiles were applied to a range of different sized scaffolds: 3x3x3; 5x5x5; and 7x7x7.

3.2 Results with constant strain profiles

Results are presented in Figure 1 for the constant strain input, with varying target stress profiles. It is evident that there are some significant variations between the target and output stress profiles for the optimised topology. This is attributed to the multivariate optimisation and the simultaneous optimisation of stress, porosity and material volume. The results of Figure 1 correspond to weighting factors in the objective function where stress, porosity and material volume have weighting factors of $\alpha = 0.4$, , $\beta = 0.4$ and $\gamma = 0.3$.

To investigate the effect of modifying the weighting factors in the objective function, the results of Figure 1b-c are reproduced in Figure 2 based on the 3x3x3 geometry, with weighting factors of $\alpha = 0.9$, $\beta = 0.05$, and $\gamma = 0.05$. These weighting factors put a higher importance on matching the target stress profile, and less importance on the target porosity and material volume.

It is evident in Figure 2 that the higher weighting on stress leads to an output stress profile significantly closer to the desired target profile. It is also evident that the larger model with more elements gives a stress distribution significantly closer to the target than the smaller lattice structures. This observation is attributed to the larger number of variables available for the optimisation in the larger model. The optimisation routine therefore has an improved ability to achieve the target stress profile. Overall these results using the synthetic stress and strain profiles validate the topology optimisation method. While there are clearly tradeoffs to be made in a multivariate optimisation such as this, the approach shows the flexibility to match different application needs for the porous lattice structures.

3.3 Results with IVD stress and strain profiles

One application of the optimisation routine is to develop orthopaedic implants for replacement of inter-vertebral discs. Work undertaken by the researchers at Colorado State University (CSU) has developed measured stress and strain profiles as references for inter-vertebral discs (Womack, Leahy et al. 2011). The work undertaken by the researchers at CSU included fresh-frozen cadaveric cervical spines, isolating the C3 to C7 segments. Strain rosettes, pressure sensors and loadcells were attached to the vertebra to allow measurement of the reaction mechanisms during the application of a compressive load.

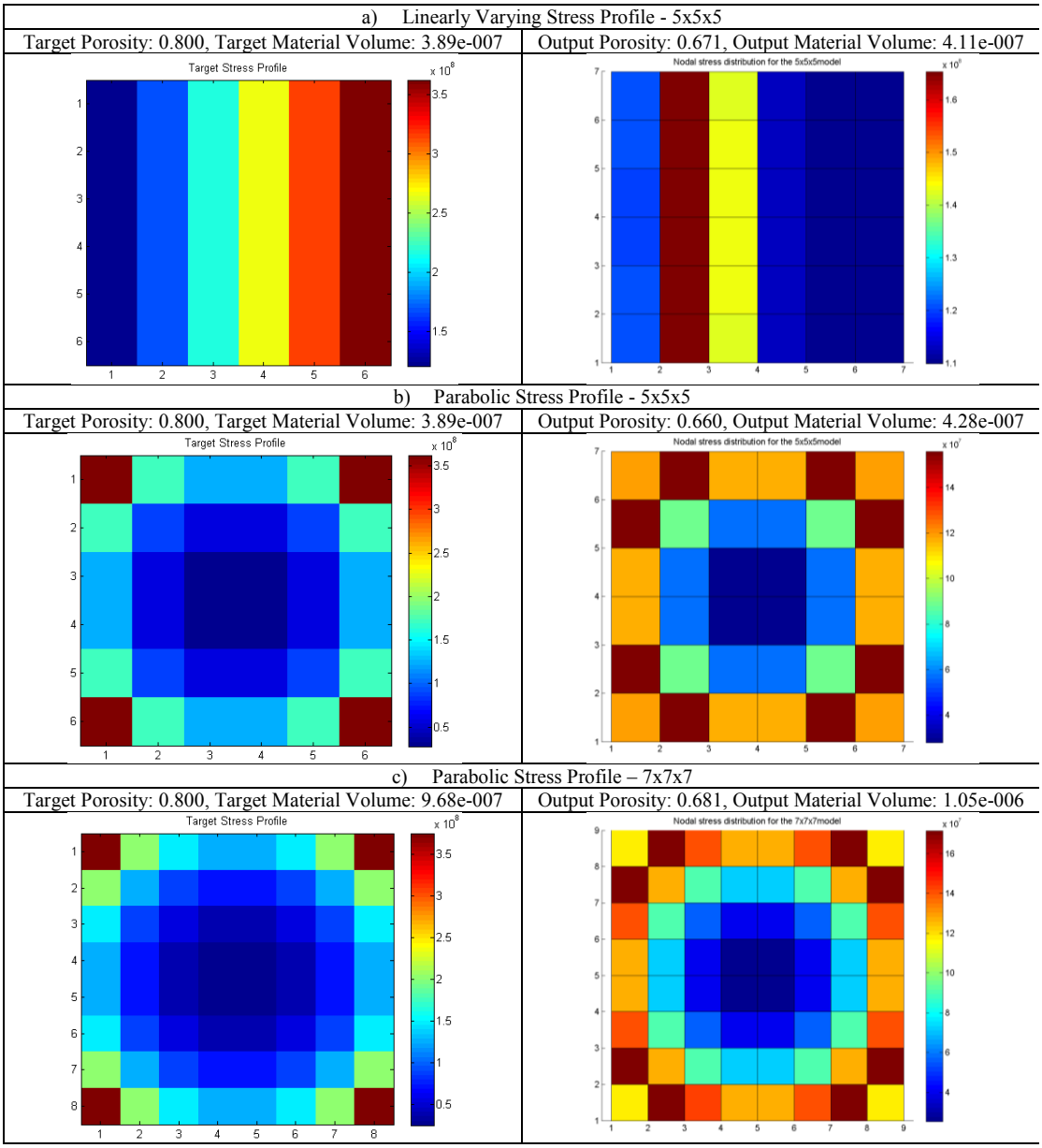

Figure 1: Results for the constant strain inputs

The measured nodal stress and strain profiles can then be interpolated onto a regular rectangular grid and incorporated within the topology optimisation routine to determine the optimal geometry to be used as an orthopaedic implant to impart similar stresses and strains into the vertebra as those resulting from the original natural disc.

Figures 3a-b present the nodal displacements and nodal stress values respectively of the IVD endplate. The prior results of the regular cubic grids using the synthetic displacement and stress profiles do not represent the proportions of an IVD. Therefore, the measured IVD displacement boundary conditions and stress target profiles presented in Figures 3 a and b are applied to a 3x14x14 grid, to more closely represent the overall size and proportions of a typical IVD. The output stress profile for the optimised geometry is presented in Figure 3c, while Figure 3d presents the output stress values on the optimised geometry. It can be seen that the porosity is approximately 25% below the target and the material volume is about 30% higher than the target. The stress output profile is very similar to the target value, indicating that the stresses imparted into the vertebra would be very close to those for a natural IVD.

Overall, the optimisation routine finds a good match, both in terms of overall stress magnitude and stress distribution across the surface of the scaffold. These results indicate that a scaffold designed using this code and then manufactured using a rapid prototyping method such as 3D printing is capable of producing biocompatible implants that can impart a stress distribution into the surrounding bone of the vertebra the can closely mimic that of a natural IVD. This outcome shows some significant promise, but future research is needed to fully test the robustness of the optimisation routine and consider more complex lattice geometries.

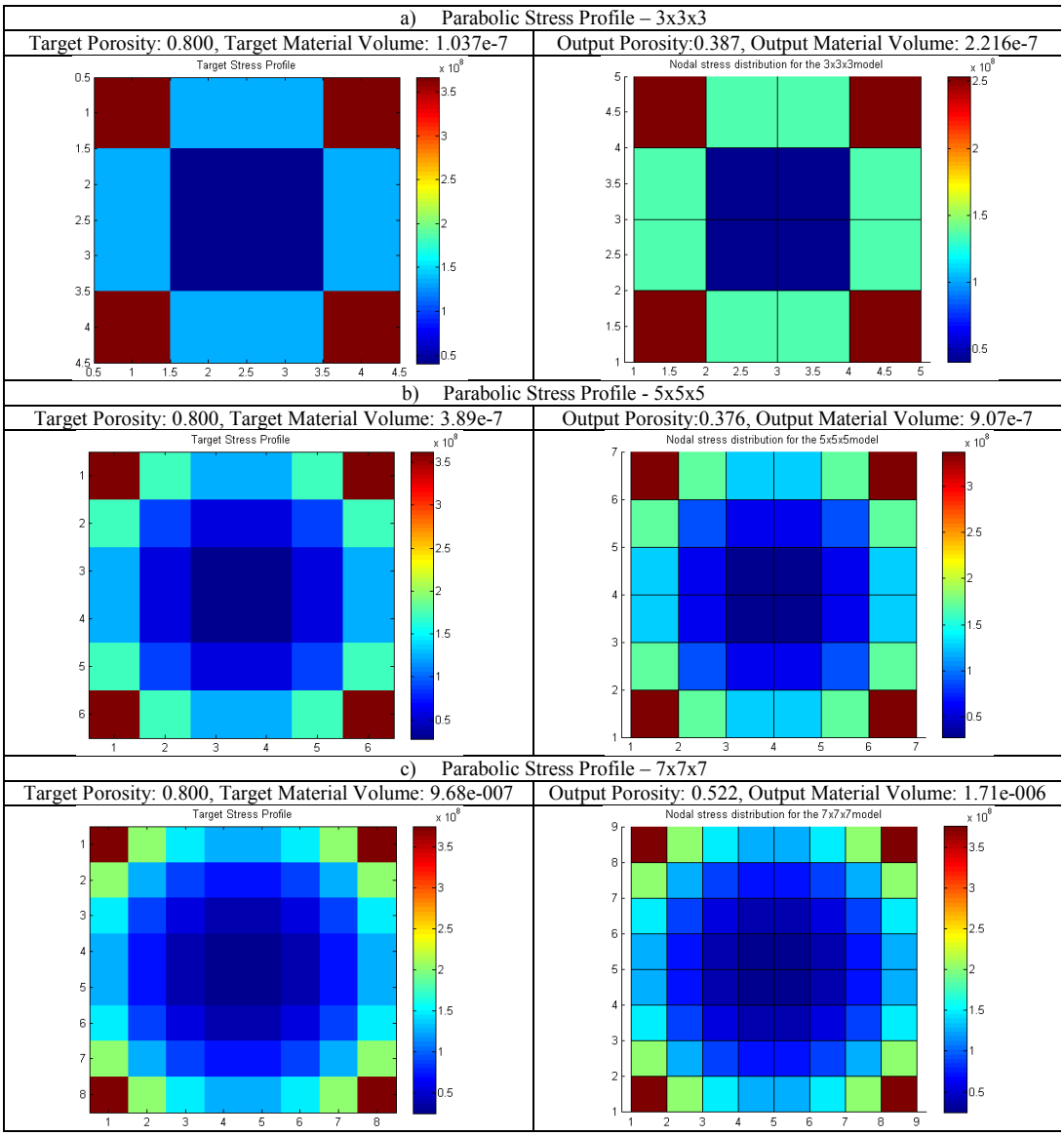

Figure 2: Results for the constant strain inputs and parabolic stress targets, with higher weighting on stress within the objective function.

3. CONCLUSIONS

This manuscript has presented some initial results on a topology optimisation routine to develop porous lattice structures that can replicate target stress and strain profiles. The ability to solve this type of design support optimization opens up a wide range of possible orthopaedic and biomedical applications to promote bone growth and osteointegration.

This manuscript has presented the key aspects of the optimisation algorithm, as well as some preliminary validation results on synthetic stress and strain profiles. The analysis is also extended to test the ability of the optimisation routine to determine geometry for human IVDs using *ex-vivo* measured values. The topology optimisation routine can be used as a design tool to guide optimal topology of orthopaedic implants.

REFERENCES:

Alvarez, K., Nakajima, H. (2009). "Metallic Scaffolds for Bone Regeneration." Materials **2**: 790-832.

Armillotta, A., Pelzer, R. (2008). "Modelling of porous structures for rapid prototyping of tissue engineering scaffolds." International Journal of Advanced Manufacturing Technology **39**: 501-511.

Ashby, M. F. (2006). "The properties of foams and lattices." Philos Transact A Math Phys Eng Sci **364**(1838): 15-30.

Ashby, M. F., Evans, A., Fleck, N.A., Gibson, L.J., Hutchison, J.W., Wadley, H.N.G. (2000). Metal Foams: A Design Guide. The United States of America, Butterworth-Heinemann.

Asholt, P. (1999). Metal Foams and Porous Metal Structures. Bremen, MIT Verlag.

Banhart, J. (2000). "Manufacturing Routes for Metallic Foams." JOM **52**(12): 22-27.

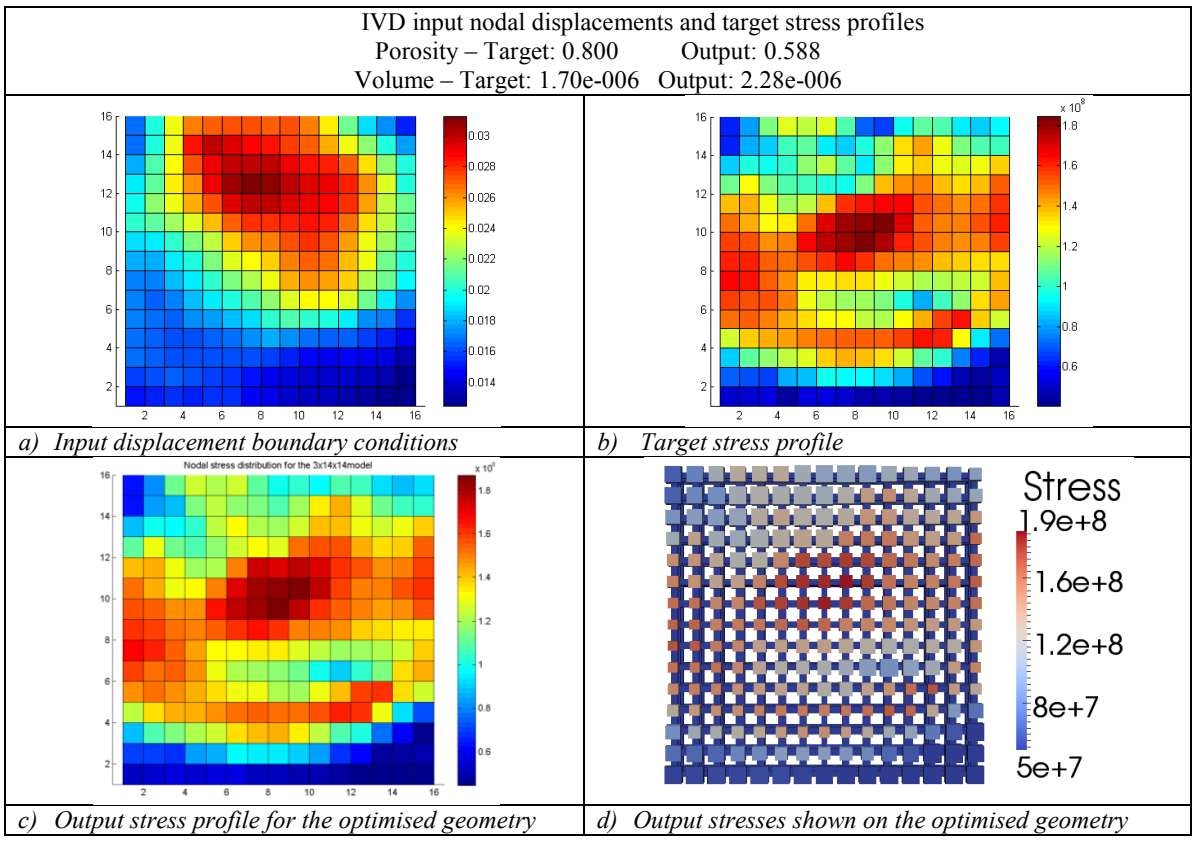

Figure 3: Results of 3x14x14 lattice geometry (the approximate IVD proportions)

Butterfield, B. G., Meylan, B.A. (1980). Three-dimensional structure of wood: an ultrastructural approach, Taylor & Francis.

Gibson, L. J., Ashby, M.F. (1997). Cellular solids : structure and properties. Cambridge, Cambridge University Press.

Hollister, S. (2005). "Porous scaffold design for tissue engineering." Nature Materials **4**(518-524).

Hollister, S. J. (2009). "Scaffold Design and Manufacturing: From Concept to Clinic." Advanced Materials **21**:3330.

Hollister, S. J., Lin, C.Y., Saito, E., Lin, C.Y., Schek, R.D., Taboas, J.M., Williams, J.M., Partee, B., Flanagan, C.L., Diggs, A., Wilke, E.N., VanLenthe, G.H., Muller, R., Wirtz, T., Das, S., Feinberg, S.E., Krebsbach, P.H. (2005). "Engineering craniofacial scaffolds." Orthodontics & Craniofacial Research **8**: 162–173.

Lefebvre, L. P., Banhart, J., Dunand, D. C. (2008). "Porous Metals and Metallic Foams: Current status and Recent Developments." Adv. Engineering Materials **10**(9): 775.

Li, Y. (2011). Wood-Polymer Composites. Advances in Composite Materials - Analysis of Natural and Man-Made Materials. P. Tesinova, InTech.

Montanini, R. (2005). "Measurement of strain rate sensitivity of aluminium foams for energy dissipation." International Journal of Mechanical Sciences **47**: 26-42.

Pietrzak, W. S., Sarver, D., Verstynen, M. (1996). "Bioresorbable Implants - Practical Considerations." Bone **19**: S109.

Prendergast, P. J. (2001). Bone Mechanics Handbook. Boca Raton, CRC Press LLC.

Rashmir-Raven, A.M., Richardson, D.C., Aberman, H.M., Young, D.J. (1995) "The response of cancellous and cortical canine bone to hydroxylapatite-coated and uncoated titanium rods." J. of Applied Biomaterials **6**: 237.

Shewchuk, J.R. (1994). An Introduction to the Conjugate Gradient Method Without the Agonizing Pain. Technical Report. Carnegie Mellon Univ., Pittsburgh, PA, USA.

Staiger, M., Pietak, A., Huadmai, J., Dias, G. (2006). "Magnesium and its alloys as orthopedic biomaterials-A review." Biomaterials **27**: 1728-1734.

Steele, D. G., Bramblett, C.A. (1988). The anatomy and biology of the human skeleton, Texas A&M University Press.

Vincent, J. F. V. (1990). Structural Biomechanics. Princeton NJ, Princeton University Press.

Wintermantel, E., Ha, S.W. (1996). Biocompatible Materials and Design: Implants for Medicine and the Environment. Biokompatible Werkstoffe und Bauweisen: Implantate fur Medizin und Umwelt. Berlin Springer

Witte, E., Ulrich, H., Rudert, M., Willbold, E. (2007). "Biodegradable magnesium scaffolds: Part 1-Appropriate inflammatory response." Journal of Biomedical Materials Research Part A **81**: 748-756.

Woesz, A. (1008). Rapid Prototying to Produce Porous Scaffolds with Controlled Architecture for Possible use in Bone Tissue Engineering. Virtual Prototyping & Bio Manufacturing in Medical Applications. B. Bidanda, Bartolo, P.J., Springer.

Womack, W., P. D. Leahy, et al. (2011). "Finite element modeling of kinematic and load transmission alterations due to cervical intervertebral disc replacement." Spine **36**(17): E1126-E1133.